Nonlinear current-voltage behavior and giant positive magnetoresistance in nonmagnetic Au/Yttria-stabilized zirconia/Si heterostructures

T. L. Qu,[1] J. Li,[1] Y. G. Zhao,[1,a)] J. W. Mei,[1] X. Liu,[1] H. F. Tian,[1] J. P. Shi,[1] S. M. Guo,[1] J. Li,[2] D. N. Zheng,[2] and J. Q. Li[2]

[1]*Department of Physics and State Key Laboratory of New Ceramics and Fine Processing, Tsinghua University, Beijing 100084, People's Republic of China*

[2]*Beijing National Laboratory for Condensed Matter Physics, Institute of Physics, Chinese Academy of Sciences, Beijing 100080, People's Republic of China*

(Received 8 September 2009; accepted 23 November 2009; published online 17 December 2009)

We report on the nonlinear current-voltage (*I-V*) behavior and giant positive magnetoresistance (GPMR) in the Au/Yttria-stabilized zirconia/Si heterostructures. The *I-V* curves of the heterostructures show a rectifying property and follow the Fowler–Nordheim tunneling behavior for the larger forward bias voltages. The GPMR of the samples increases with decreasing temperature and exceeds 100 000% in a magnetic field of 7 T at 20 K with a voltage of +4 V. It also shows anisotropy with magnetoresistance for the magnetic field perpendicular to the current larger than that of the parallel case. A possible mechanism was proposed to account for the results. © *2009 American Institute of Physics*. [doi:10.1063/1.3274130]

There is an on-going interest in the giant positive magnetoresistance (GPMR) effects in nonmagnetic materials because of their importance for the understanding of carrier transport in magnetic fields as well as applications.[1–6] GPMR effects have been observed in the silver chalcogenides,[1] single-crystal bismuth thin films,[2] inhomogeneous narrow-gap semiconductors,[3] lightly phosphorus doped silicon,[4] etc. Recently, GPMR effects were also observed in a few nonmagnetic heterostructures which show nonlinear current-voltage (*I-V*) behavior, such as the $Si-SiO_2-Al$ (Ref. 5) and multilayer ZnO/SiO_2 system.[6] Mechanisms involving magnetic field induced postponement of onset of impact ionization to higher electric fields[5] and Aharonov–Casher effect[6] have been proposed to account for the GPMR effects in the nonmagnetic heterostructures. Yttria-stabilized zirconia (YSZ) is widely used as a dielectric insulator with a large bandgap of 7.8 eV and high dielectric constant of 25.[7] In this letter, we report on the nonlinear *I-V* characteristics and GPMR effect in the nonmagnetic Au/YSZ/Si heterostructures. The GPMR increases with decreasing temperature and shows strong anisotropy at low temperatures. Analysis of the results suggests that the GPMR effect originates from the impact of magnetic field on the trap assisted Fowler–Nordheim (FN) tunneling of the heterostructures.

YSZ film was grown on the Sb heavily doped n-type (100) silicon substrate (0.02 Ω cm and 1×10^{17} cm^{-3}) by pulsed laser deposition.[8] The oxygen pressure was set to 5×10^{-4} Pa and the substrate temperature was kept at 820 °C during deposition. The energy density of the laser pulse was about 1.5 J/cm^2 and the repetition rate was 7 Hz. After deposition, the film was cooled down in the background vacuum. Then gold pads with an area of 0.25 mm^2 were grown on YSZ film and the bottom of silicon substrate as electrodes by magnetron sputtering. X-ray diffraction pattern of the sample indicates (001) orientation of YSZ film as shown in Fig. 1(a). The structural examination of this heterostructure was also performed by using a Tecnai-F20 (200 kV) transmission electron microscope (TEM). Samples for cross-section TEM observation were prepared by the conventional method consisting of gluing, cutting, mechanical polishing, dimpling, and finally ion thinning. The current-voltage (*I-V*) characteristics at different magnetic fields and temperatures were measured via two-probe method by a Keithley 2400 sourcemeter in an environment supplied by quantum design magnetic property measurement system (MPMS-XL7).

A low magnification bight-field TEM image of the Si/YSZ heterostructure was shown in Fig. 1(b), which clearly exhibits the uniform and continuous YSZ film with a thickness of 160 nm. The inset of Fig. 1(b) illustrates a corresponding high-resolution TEM image showing the atomic structure in the Si/YSZ interface region. No evidence of SiO_2

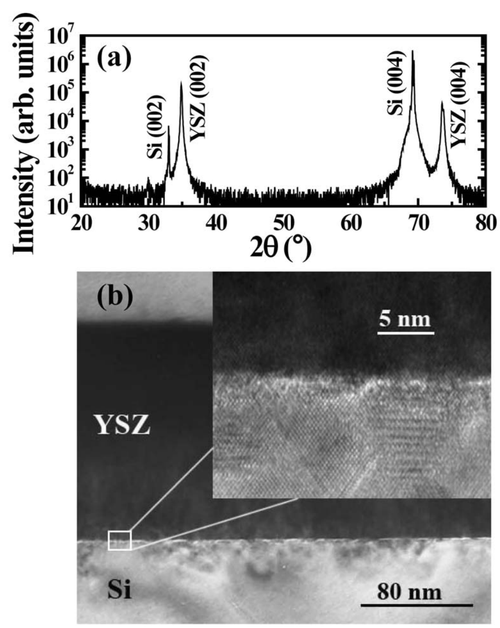

FIG. 1. (a) X-ray diffraction pattern for YSZ/Si heterostructures. (b) The cross-section TEM image of YSZ/Si heterostructures. The inset is the high-resolution TEM image near the interface.

a)Electronic mail: ygzhao@tsinghua.edu.cn.

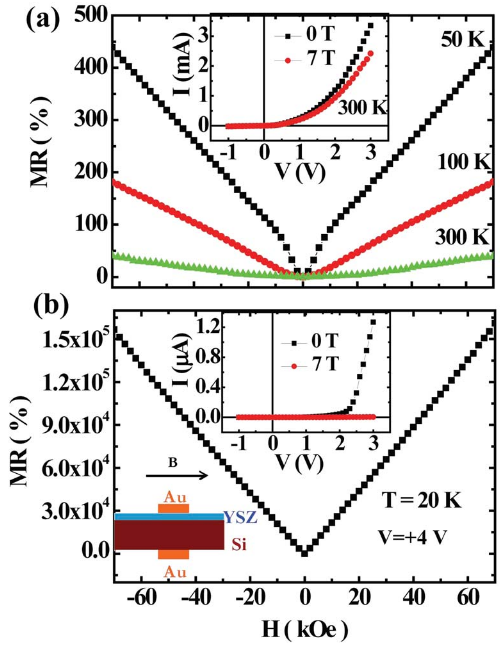

FIG. 2. (Color online) MR as a function of the magnetic field for Au/YSZ/Si heterostructures at 300, 100, and 50 K (a) and 20 K with a forward bias voltage of 4 V (b). The insets are the *I-V* curves measured at 300 K (a) and 20 K (b) with $B=0$ and 7 T, respectively.

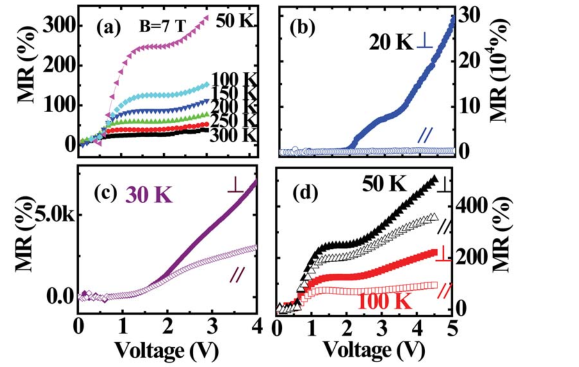

FIG. 3. (Color online) (a) Forward bias voltage dependence of MR at different temperatures in a magnetic field of 7 T. (b), (c), (d) show MR vs voltage at 20, 30, 50, and 100 K with magnetic field perpendicular and parallel to the current, respectively.

layer is found between YSZ film and Si substrate, which is consistent with the previous report.[7]

Figure 2(a) shows the nonlinear *I-V* characteristics and GPMR of the Au/YSZ/Si heterostructures at different temperatures with a forward bias voltage of 4 V. The left inset in Fig. 2(b) schematically illustrates the electrode settings where the forward bias corresponds to the application of a positive voltage on the top Au electrode and the magnetic field is parallel to the sample surface. The *I-V* curves exhibit a rectifying property and are highly nonlinear. The junction current increases dramatically with increasing forward bias voltage but remains low for the reverse bias voltages. The most interesting result is the GPMR as shown in the inset of Fig. 2 by the large separation between the two *I-V* curves measured in magnetic fields of 0 and 7 T, respectively. Magnetoresistance (MR) is defined as $[R_j(H)/R_j(0)-1]\times 100\%$ for a certain voltage, where R_j is the junction resistance (V/I) for the voltage, $R_j(0)$ and $R_j(H)$ are the resistances without and with an applied field, respectively. The MR of the samples was measured at different temperatures with a forward bias voltage of 4 V and magnetic field sweeping from −7 to 7 T. As shown in Fig. 2, MR increases dramatically with increasing magnetic field without the sign of saturation. In a magnetic field of 7 T and with a forward bias voltage of 4 V, MR can reach 160 000% at 20 K and 40% at 300 K. In order to find the origin of the GPMR effect, we also measured the out-of-plane *I-V* characteristics of the Au/Si/Au between 5 and 300 K, no MR was found. Furthermore, the resistance of Au/YSZ/Si structure is much larger (at least two orders) than that of Au/Si/Au in the whole temperature range. Therefore, the MR effect in Au/YSZ/Si M-I-S structure should be related to the structure rather than the Si substrate itself.

To understand the GPMR effect, we present the forward bias voltage dependence of MR in a magnetic field of 7 T at different temperatures in Fig. 3(a). MR starts to increase rapidly with bias voltage at a certain voltage and then shows a minor decrease, followed by another increase with bias voltage. In contrast, no MR effect was observed for the reverse bias. Figures 3(b)–3(d) show MR versus V at 20, 30, 50, and 100 K, respectively, with magnetic field perpendicular ($\perp$) and parallel ($\parallel$) to the current. It can be seen that $MR_{\perp}$ is larger than $MR_{\parallel}$. This anisotropy of MR exists for all temperatures and is more remarkable at low temperatures. It should be mentioned that our work is different from that of Schoonus *et al.*[5] in the following aspects. First, they studied the $Al/SiO_2/Si/SiO_2/Al$ structure with lightly doped Si and only the backward *I-V* characteristics could be measured because the symmetry of the structure. While we studied the Au/YSZ/Si heterostructures with heavily doped Si and MR effect was only observed in the forward *I-V* characteristics. Second, they only observed MR below 36 K and MR does not show anisotropy. In contrast, we observe MR from room temperature to low temperatures and the MR shows anisotropy. Third, as they proposed, the MR in their work is due to the effect of magnetic field on the impact ionization of the acceptors, which is quite different from the present work as shown later.

In order to understand the GPMR in Au/YSZ/Si heterostructures, we also have to know the electronic transport mechanism in the heterostructures, which can be deduced from the *I-V* characteristics of the samples at different temperatures. Figure 4(a) shows the *I-V* curves plotted with $\ln(J/V^2)$ versus $1/V$ at different temperatures for the forward bias voltages. The linear behavior in the high voltage range is a signature of the FN tunneling through a triangular potential barrier,[9] which is a usual leakage current mechanism in the relatively thick insulating layer under a strong electric field.[9–13] The FN tunneling current is $J_V=(CV^2/d^2\phi_0)\exp[-\lambda(d\phi_0^{3/2}/V)]$, where C, λ are constants and V, d, and ϕ_0 are applied voltage, thickness of the insulating film, and effective barrier height, respectively.[9] The different slopes correspond to the different tunneling barrier heights ϕ_0 [see Fig. 4(c)] for different temperatures. As shown in Fig. 4(b), the plot of $d/dV[\log(dI/dV)]$ versus V shows a peak, whose voltage V_{peak} corresponds to the tunneling barrier height ϕ_0 with $\phi_0=eV_{peak}$.[10] Thus, ϕ_0 increases with decreasing temperature, from 0.2 eV at 300 K to 0.6 eV at 30 K, which is consistent with the temperature dependence of the slopes of $\ln(J/V^2)$ versus $1/V$ since the slope is equal

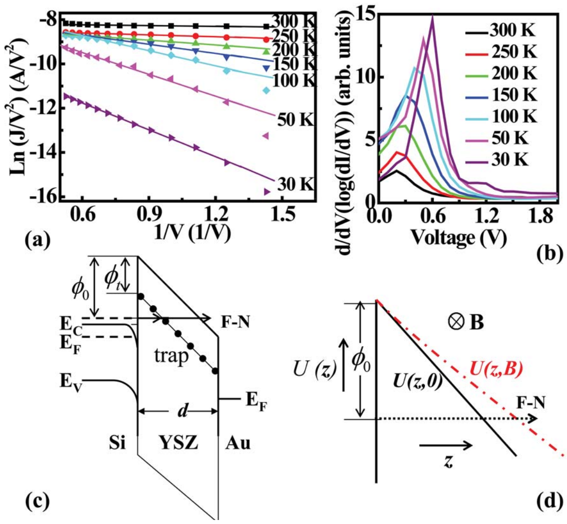

FIG. 4. (Color online) (a) I-V curves plotted as $\ln(J/V^2)$ vs $1/V$ at different temperatures. (b) $d/dV[\log(dI/dV)]$ vs V. (c) The schematic band diagram of Au/YSZ/Si heterostructure for the trap-assisted FN tunneling. (d) A schematic diagram for electron tunneling through a triangular barrier with and without a magnetic field.

to $-\lambda d\phi_0^{3/2}$. Furthermore, the barrier height ϕ_0 is relatively lower than that of an ideal YSZ tunneling barrier (1.4 eV) (Ref. 14) and this difference may be related to the traps in YSZ layer which are generated due to the high vacuum during the deposition process.[7] In fact, when the insulator contains a non-negligible number of traps, the tunnel emission will be dominated by field ionization of trapped electrons into the conduction band of the dielectric.[11] If the conduction is mainly due to the tunneling of trapped electrons, the current density equation is the same as FN tunneling with the interfacial barrier height ϕ_0 replaced by the trap barrier height ϕ_t [see Fig. 4(c)].[11,12] In this scenario, electrons at the interface of YSZ/Si can tunnel through the triangular barrier into the conduction band of YSZ assisted by traps in YSZ as shown in Fig. 4(c).

Now, we try to understand why magnetic field can dramatically suppress the current of Au/YSZ/Si heterojunctions, leading to the GPMR effect. For FN tunneling process, electron faces a triangular barrier [see Fig. 4(c) and 4(d)] which can be expressed as

$$U(z,0) = \phi_0 - Az, \tag{1}$$

where ϕ_0 is the abrupt barrier height between Si and YSZ, $A = eV/d$ and z is the space coordinate along the tunneling direction. When a magnetic field is applied perpendicular to the tunneling direction, a "magnetic barrier" $m\omega_c^2 z^2/2$ emerges,[15] then the barrier changes to

$$U(z,B) = U(z,0) + \tfrac{1}{2}m\omega_c^2 z^2, \tag{2}$$

as shown in Fig. 4(d), where ω_c ($\omega_c = eB/m$) is the cyclotron frequency. Based on the theory of Wentzel-Kramers-Brillouin (WKB) approximation, we know that, due to the magnetic barrier, the tunneling electron has to face a higher barrier and tunnel through a longer distance, thus the tunneling probability decreases in a magnetic field. To explain why the magnetic field can have a strong effect on the tunneling process, we estimated the lifetime τ and the ω_c of the tunneling electron. For a triangular barrier [see Fig. 4(d)] in our heterostructure, the lifetime τ for the tunneling electron can be calculated by using $\tau \simeq \int_0^z dz/\sqrt{2[U(z)-E]/m} = \sqrt{2m}[d(\phi_0-E)^{1/2}/eV]$ (Ref. 16). With $\phi_0 = 0.5$ eV, $U(z) = \phi_0 - Az$, $A = eV/d$, $E = 0$, $d = 160$ nm, $m^* = 0.2m_e$, $V = 1$ V, and B=7 T, we obtain $\tau \simeq 1.7 \times 10^{-13}$ s. In addition, $\omega_c = eB/m = 6.2 \times 10^{12}$ Hz, which satisfies $\omega_c^* \tau \geq 1$, thus the magnetic field effect is strong for electron tunneling process.[16] At low temperatures, the lifetime increases due to the increase in ϕ_0, so the MR is larger. In the above analysis, we only considered the magnetic field perpendicular to the tunneling direction. The MR effects for magnetic field parallel to the current direction is expected to be much small compared with the perpendicular case. This is consistent with the strong anisotropy of MR for the heterostructures, especially at low temperatures.

We thank Ping Ao, G. M. Zhang, and Y. Xu for stimulating discussions. This work was supported by the National Natural Science Foundation of China (Grant Nos. 10674079 and 50628202), Ministry of Science and Technology of China (Grant No. 2006CB921502), and Specialized Research for the Doctoral Program of Higher Education.

[1] R. Xu, A. Husmann, T. F. Rosenbaum, M. L. Saboungi, J. E. Enderby, and P. B. Littlewood, Nature (London) **390**, 57 (1997).
[2] F. Y. Yang, K. Liu, K. M. Hong, D. H. Reich, P. C. Searson, and C. L. Chien, Science **284**, 1335 (1999).
[3] S. A. Solin, T. Thio, D. R. Hines, and J. J. Heremans, Science **289**, 1530 (2000).
[4] M. P. Delmo, S. Yamamoto, S. Kasai, T. Ono, and K. Kobayashi, Nature (London) **457**, 1112 (2009).
[5] J. J. H. M. Schoonus, F. L. Bloom, W. Wagemans, H. J. M. Swagten, and B. Koopmans, Phys. Rev. Lett. **100**, 127202 (2008).
[6] S. Miyanishi, M. Yagura, N. Teraguchi, K. Shirakawa, K. Sakuno, Y. Murakami, K. Kojima, A. Takahashi, and K. Ohta, Appl. Phys. Lett. **91**, 192104 (2007).
[7] S. J. Wang, C. K. Ong, S. Y. Xu, and P. Chen, Appl. Phys. Lett. **78**, 1604 (2001).
[8] J. Li, P. Wang, J. Y. Xiang, X. H. Zhu, W. Peng, F. Y. Chen, D. N. Zheng, and Z. W. Li, Appl. Phys. Lett. **86**, 112514 (2005).
[9] M. Lenzlinger and E. H. Snow, J. Appl. Phys. **40**, 278 (1969).
[10] T. Nagahama, T. S. Santos, and J. S. Moodera, Phys. Rev. Lett. **99**, 016602 (2007).
[11] S. M. Sze, *Physics of Semiconductor Devices*, 2nd ed. (Wiley, New York, 1981); S. M. Sze, J. Appl. Phys. **38**, 2951 (1967).
[12] K. Y. Lim, D. G. Park, H. J. Cho, J. J. Kim, J. M. Yang, I. S. Choi, I. S. Yeo, and J. W. Park, J. Appl. Phys. **91**, 414 (2002); X. R. Cheng, Y. C. Cheng, and B. Y. Liu, *ibid.* **63**, 797 (1988).
[13] I. D. Parker, J. Appl. Phys. **75**, 1656 (1994); I. Musa, D. A. I. Munindrasdasa, G. A. J. Amaratunga, and W. Eccleston, Nature (London) **395**, 362 (1998); T. Sugino, C. Kimura, and T. Yamamoto, Appl. Phys. Lett. **80**, 3602 (2002); S. Barth, U. Wolf, H. Bassler, P. Muller, H. Riel, H. Vestweber, P. F. Seidler, and W. Rie, Phys. Rev. B **60**, 8791 (1999); I. Stolichnov, A. K. Tagantsev, E. L. Colla, and N. Setter, Appl. Phys. Lett. **73**, 1361 (1998).
[14] Y.-Y. Fan, R. E. Nieh, and J. C. Lee, IEEE Trans. Electron Devices **49**, 1969 (2002).
[15] T. Sharpee, M. I. Dykman, and P. M. Platzman, Phys. Rev. B **64**, 245309 (2001).
[16] This is the time scale that enters in most tunneling problems. For a review see E. H. Hauge and J. A. Støvneng, Rev. Mod. Phys. **61**, 917 (1989).